Journal of Hydrology 475 (2012) 379–391

Contents lists available at SciVerse ScienceDirect

Journal of Hydrology

journal homepage: www.elsevier.com/locate/jhydrol

Rainfall–runoff modeling of recent hydroclimatic change in a subtropical lake catchment: Laguna Mar Chiquita, Argentina

Magali Troin [a,*], Christine Vallet-Coulomb [a], Eduardo Piovano [b], Florence Sylvestre [a]

[a] CEREGE, Aix-Marseille Université, CNRS, IRD, Europôle méditerranéen de l'Arbois, BP 80, 13545 Aix-en-Provence cedex 4, France
[b] CICTERRA-CIGeS, Universidad Nacional de Córdoba, Av. Velez Sarsfield 1611, X5016GCA Córdoba, Argentina

ARTICLE INFO

Article history:
Received 5 June 2012
Received in revised form 28 August 2012
Accepted 13 October 2012
Available online 30 October 2012
This manuscript was handled by Konstantine P. Georgakakos, Editor-in-Chief, with the assistance of Raymond Najjar, Associate Editor

Keywords:
SWAT
Parameter transferability
Climate change
Land cover change
Lake level variations
Southeastern South America

SUMMARY

The 1970s abrupt lake level rise of Laguna Mar Chiquita in central Argentina was shown to be driven by an increase in the Rio Sali-Dulce discharge outflowing from the northern part of the lake catchment. This regional hydrological change was consistent with the 20th century hydroclimatic trends observed in southeastern South America. However, little is known about the impacts of climate or land cover changes on this regional hydrological change causing the sharp lake level rise. To address this question, the present study aims to provide an integrated basin-lake model. We used the physically-based SWAT model in order to simulate streamflow in the Sali-Dulce Basin. The ability of SWAT to simulate non-stationary hydrological conditions was evaluated by a cross-calibration exercise. Based on observed daily meteorological data over 1973–2004, two successive 9-year periods referred to as wet ($P_{1976–1985}$ = 1205 mm/yr) and dry ($P_{1986–1995}$ = 796 mm/yr) periods were selected. The calibration yielded similar Nash–Sutcliffe efficiencies (*NSE*) at the monthly time scale for both periods (NSE_{wet} = 0.86; NSE_{dry} = 0.90) supporting the model's ability to adapt its structure to changing climatic situations. The simulation was extended in scarce data conditions over 1931–1972 and the simulation of monthly discharge values was acceptable (*NSE* = 0.71). When precipitation in the model was increased until it reach the change observed in the 1970s ($\Delta P/\overline{P} = 22\%$), the resulting increase in streamflow was found to closely match the 1970s hydrological change ($\Delta Q/\overline{Q} = 45\%$). Sensitivity analyses revealed that the land cover changes had a minor impact on the 1970s hydrological changes in the Sali-Dulce Basin. Integrating the SWAT simulations within the lake model over 1973–2004 provided lake level variations similar to those obtained using observed discharge values. Over the longer period, going back to 1931, the main features of lake levels were still adequately reproduced, which suggests that this basin-lake model is a promising approach for simulating long-term lake level fluctuations in response to climate.

1. Introduction

The southeastern South America (SESA) region was affected by a major hydroclimatic change at the beginning of the 1970s (Garcia and Mechoso, 2005; Pasquini et al., 2006). A wet phase characterized by high precipitation and increased river discharges was recorded and has widely affected the subtropical plains of South America (Garcia and Vargas, 1998). It is therefore critical to understand this recent hydroclimatic transition and its environmental impacts (Garcia and Vargas, 1998; Garcia and Mechoso, 2005; Pasquini et al., 2006), particularly as this region is highly dependent on agriculture and hydroelectricity.

In central Argentina, Laguna Mar Chiquita (30°54′S–62°51′W), the largest saline lake in South America, saw its level increase sharply in the 1970s and has clearly undergone the major 20th century hydroclimatic change recorded in SESA. Lake sediment studies have revealed that this hydrological change is probably one of the most important over the last millennium and have demonstrated that Laguna Mar Chiquita is a sensitive recorder of hydrological variations at different time scales in SESA (Piovano et al., 2009). Understanding the links between lake level fluctuations and climate variability through a modeling approach thus provides an opportunity to explore the relationships between climate and regional water balance. In particular, a modeling approach can allow a better assessment of the relative impacts of climate change on water resources in the region. In that scope, a recent modeling study was conducted to quantify the water balance of Laguna Mar Chiquita and to assess the sensitivity of lake levels to water balance components (Troin et al., 2010). The results showed that the abrupt lake level rise in 1973 was driven by an increase in the Rio Sali-Dulce discharge stemming from the northern part of the lake catchment. One interesting point raised by this study was the fact that the Sali-Dulce Basin, which only covered 19% of the total lake

* Corresponding author. Tel.: +33 (0) 4 42 97 15 89; fax: +33 (0) 4 42 97 15 95.
E-mail address: troin@cerege.fr (M. Troin).

0022-1694/$ - see front matter © 2012 Elsevier B.V. All rights reserved.
http://dx.doi.org/10.1016/j.jhydrol.2012.10.010

catchment area (estimated as 127,000 km^2) was responsible for 92% of the 1970s lake level rise (Troin et al., 2010). In the present study, the main objective is to use a physically-based distributed hydrological model to simulate streamflow in the Sali-Dulce Basin in order to provide an integrated basin-lake model able to reproduce the hydroclimatic transition of the 1970s. Since this region of Argentina also encountered an important expansion of cultivated areas in the early 1970s due to increasing population (Hall et al., 1992; Magrin et al., 2005), our hydrological modeling approach can help assess the respective roles of land cover and climate changes on the catchment's streamflow.

Generally, physically-based distributed models are preferred for simulating rainfall–runoff relationships under changing climatic conditions due to their sound description of hydrological processes and their ability to incorporate basin heterogeneity and the spatial distribution of climate variables (Legesse et al., 2003, 2010; Setegn et al., 2010). However, the main drawbacks to the application of these models stem from their high demand in input data (Leavesley, 1994; Anderson et al., 2006; Borman, 2008). The lack of both meteorological and hydrological data is well-known in SESA (Stehr et al., 2008). In central Argentina, the meteorological station network is not very dense, data duration is quite short and there are many missing data values. In addition, the hydrological data necessary to calibrate and validate models are scarce and available at monthly time step only. To overcome the short-comings of the meteorological time series, some physically-based distributed models such as the Soil Water Assessment Tool (SWAT) model (Arnold et al., 1998) have developed their own weather generator (WXGEN; Sharpley and Williams, 1990). Since precipitation is a major driver of hydrologic responses (Beven, 2004; Bardossy and Das, 2008), the accuracy of the precipitation values calculated by the weather generator has to be evaluated prior to the modeling approach. In particular, the statistical properties of generated precipitation need to be examined before the implementation of the hydrological model and alternative methods have to be considered for reconstructing missing data.

The purpose of hydrological studies is often to investigate the ability of models to simulate streamflow under current climatic conditions, prior to extending their application to past and/or future climate conditions. An important concern to such hydrological modeling applications is to determine the ability of a catchment model to properly reproduce streamflow for a large range of climatic situations (Leavesley, 1994). In that scope, Klemes (1986) suggested a hierarchical scheme for testing the climatic transferability of hydrological models based on cross-calibration experiments. Although a few recent studies have explicitly used this procedure for meso-scale catchments (Apaydin et al., 2006; Shrestha et al., 2007), this type of modeling approach is still largely unexplored because of the lack of long-term hydroclimatic time series covering changing climatic conditions.

In this context, this study focuses on the evaluation of SWAT's ability to simulate non-stationary conditions in a region of South America characterized by a major hydroclimatic change from dry to wetter conditions. SWAT was developed at the United States Department of Agriculture (USDA) by Arnold et al. (1998) and is one of the most commonly used watershed model worldwide to assess the impacts of land cover and climatic changes on hydrologic cycles (Neitsch et al., 2002; Gassman et al., 2007; Borman et al., 2007; Abdo et al., 2009). The first step of this study is to select the relevant method to fill gaps in meteorological time series. Aside from the weather generator included in SWAT, alternative methods such as statistical correlation methods are examined. Secondly, the ability of SWAT to simulate streamflow under changing climatic conditions is evaluated. As such, a cross-calibration experiment is performed in order to analyse the transferability of model parameters. The SWAT simulation is then extended over the recent past and scenario simulations are performed to determine the respective roles of climate and land cover changes on the 1970s hydrological change in the Sali-Dulce Basin. To this end, the SWAT simulation is integrated in the lake model in order to evaluate the performance of the overall basin-lake model at reproducing the main trends of lake level variations in the hopes of better understanding and simulating long-term lake level fluctuations in response to climate.

2. General description of the study area

Located in the northwestern part of the Laguna Mar Chiquita catchment (127,000 km^2 from 26°S to 32°S and 62°W to 66°W; Fig. 1), the Sali-Dulce Basin spans an area of 23,810 km^2 from 26° to 28°S and from 64° to 66°W. This watershed is part the Chaco-Pampean Plain and occupies a tectonic depression formed during the middle Pleistocene (Kröhling and Iriondo, 1999). Its topographic relief has elevations ranging from 222 m in the plain, to 1500 m in the humid piedmonts and up to 5400 m on the arid moutainous borders (Fig. 1).

The Sali-Dulce Basin is the collector of many rivers coming from the western arid moutainous borders (Fig. 1). It forms an alluvial fan extending over a plain with a low gradient until the Rio Hondo reservoir. The Rio Hondo reservoir is a large and flat water impoundment (S = 330 km^2, depth = 40 m) created in 1967 for water flow regulation and hydropower generation. Over the Sali-Dulce Basin, the unconfined aquifer occupies most of the basin up to 20 m below the surface (Garcia et al., 2006). It is characterized by loessic sediments interbedded with sandy channels and is mostly recharged by precipitation infiltration (Figueroa et al., 1996). The shallow aquifer of the Sali-Dulce Basin plays an important regional socio-economic role in providing water necessary to local communities.

Climate conditions in the Sali-Dulce Basin present long rainy summers and mild dry winters. The annual average daily temperature ranges from 13 to 20 °C between May and September and from 21 to 28 °C between December and March with an annual mean of 20 °C. The coldest and warmest months are July and January respectively. The rainy season extends from December to March and the dry season extends from May to September. The mean annual rainfall of the catchment area is about 993 mm. The atmospheric circulation is characterized by northeasterly and easterly moisture-bearing winds that develop in response to a seasonal low-pressure system east of the Andes. The low-pressure cell also attracts air masses from the Pacific Anticyclone generating dry and cold winds which gain intensity during the austral winter (Prohaska, 1976; Hastenrath, 1991). Precipitation within the basin is highly seasonal. Austral summer precipitation is associated with convection and winter precipitation with equator-ward moving cold fronts (Lenters and Cook, 1999). Orographic precipitation from dominant easterly and northeasterly winds exceeding 1500 mm per year occur in the northern part of the basin. The center of the Sali-Dulce Basin receives less precipitation and is characterized by sparse vegetation cover (Galvan, 1981; Bianchi and Yañez, 1992).

3. Hydroclimatic changes over 1931–2004

3.1. Meteorological and hydrological data

The National Climatic Data Center (NCDC) and the CLARIS LPB project database (http://www.claris-eu.org/) provided daily precipitation as well as daily minimum and maximum temperatures within the basin. These data come from five stations that cover the 1973–2004 period over the watershed (Fig. 1). Station 5 also

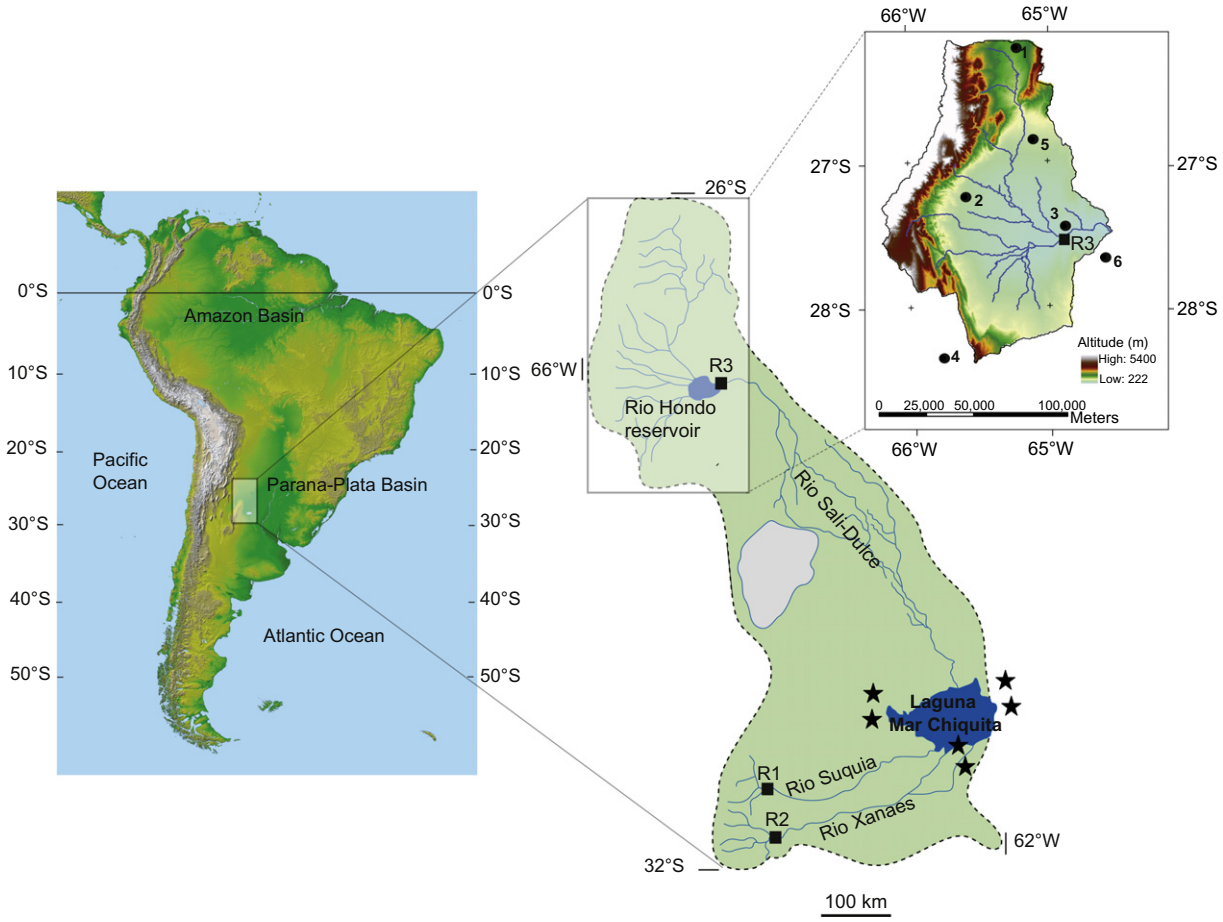

Fig. 1. Location of Laguna Mar Chiquita Basin at the west of the Paraná-Plata Basin. The enlarged view shows the Sali-Dulce Basin in the northern part of the lake basin. Data used for SWAT come from meteorological stations 1 to 6 and gauging stations R3 at the Rio Hondo reservoir outlet. Data from 6 meteorological stations around the lake (black stars) and 3 gauging stations (R1, R2, R3) were used for the lake water balance model (Troin et al., 2010).

provides data starting in 1931. The data from an additional station (6) is used for the 1931–1972 period (Fig. 1 and Table 1).

The Laboratorio de Hidráulica at the Universidad Nacional de Córdoba provided monthly discharge for the 1931–2004 period at the Hondo Station located below the Rio Hondo reservoir. A complete time series is obtained by combining two neighboring gauging stations well correlated over the 1967–1982 period ($r^2 = 0.99$). The corresponding drainage area represents 98% of the Sali-Dulce Basin area (Fig. 1 and Table 2).

3.2. Replacement of missing meteorological data

Across the stations, 12% of the daily precipitation and 13% of the temperature data (on average) are unavailable over the 1973–2004 period (Table 1). Minimum and maximum temperature data are occasionally missing for any given day from 1973 to 2004. The missing values in temperatures would exert a limited influence, if any, on long-term simulation results. The weather generator (WXGEN) program included in SWAT (Sharpley and Williams, 1990) is selected to fill-in occasionally missing daily temperature data. Missing precipitation data duration extend from 1 day to nine consecutive years (e.g. station 5). Compared to the influence of missing temperature data, the influence of missing precipitation data would be more significant on simulated streamflow. WXGEN fills precipitation gaps based on monthly statistics calculated using available long series of daily precipitation; its performance is not expected to be optimum if little daily data is available. Alternative statistical methods that were proven suitable for sparse data (Schuol et al., 2008) or non-stationary climatic conditions (the situation of interest for the present study) are compared to WXGEN for reconstructing missing daily precipitation data. Statistical correlation methods are applied assuming that well-correlated stations indicate similar inter-annual precipitation variability. Missing daily precipitation data is estimated from the normal ratio method based on one reference station using monthly ratios as follows,

$$P_{d,i} = \left(\frac{P_{m,i}}{P_{m,r}}\right) P_{d,r} \quad (1)$$

where $P_{d,i}$ is the generated daily precipitation at station i (mm of water); $P_{m,i}$ and $P_{m,r}$ are, respectively, the monthly mean precipitation at station i and at the reference station r for the month m calculated over their common observation period (mm of water); and $P_{d,r}$ is the daily precipitation at the reference station r (mm of water). This is a standard method in climatology (Paulhus and Kohler, 1952) and is frequently used to correct reanalysis precipitation data (Qian et al., 2006).

To identify the statistical significance of trends in monthly time series of precipitation between stations, the analysis is confined to a non-parametric statistical test. Spearman's rank correlation coefficient (r) is used to detect the existence of relationships between stations. Of the five meteorological stations that cover the 1973–2004 period, three stations exhibited significant

Table 1
The name, location and main characteristics of the six meteorological stations (bracket values refer to the standard deviation of annual precipitation).

	Station	Elevation (m)	Latitude (S)	Longitude (W)	1931–1972 time period				1973–2004 time period					
					Annual rainfall (mm)	Proportion of daily missing data (%)	Average minimum temperature (°C)	Average maximum temperature (°C)	Annual rainfall (mm)	Proportion of daily missing data (%)	Average minimum temperature (°C)	Average maximum temperature (°C)	Proportion of daily missing data (%)
1	Lules	950	26.21	65.21	–	–	–	–	1621 (549)	6	14.2	26.5	23
2	Las Canas	1300	27.24	65.59	–	–	–	–	1091 (244)	0.3[a]	13.9	27.5	18
3	Las Termas	281	27.45	64.89	–	–	–	–	406 (201)	16	13.7	28	0.9
4	Catamarca	464	28.35	65.77	–	–	–	–	673 (256)	7	14.3	28.4	0.3
5	Tucuman	455	26.85	65.09	946 (233)	0	17.7	26.2	1175 (325)	30	14	27.2	24
6	Santiago del Estero	20	27.67	64.60	512 (137)	0.2	13.4	28.2	–	–	–	–	–

[a] The daily missing precipitation data for the station 2 occur only during December, 2004.

correlations at the monthly time scale, i.e. station 1 *versus* station 2 ($n = 361$, $r = 0.88$, p-value = 0.01) and station 1 *versus* station 3 ($n = 311$, $r = 0.83$, p-value = 0.01); lower correlations are found for stations 4 and 5 (i.e. r values stay between 0.53 and 0.69). The missing precipitation values for those two stations are reconstructed using multiple regressions based on two reference stations as follows,

$$P_{d,i} = a_{m,r1} \times P_{d,r1} + a_{m,r2} \times P_{d,r2} \quad (2)$$

where $P_{d,i}$ is the daily precipitation at station i (mm of water); $P_{d,r1}$ and $P_{d,r2}$ are, respectively, the daily precipitation at the two reference stations $r1$ and $r2$ (mm of water); and $a_{m,r1}$ and $a_{m,r2}$ are the regression coefficients determined for each month ($m = 1$–12) by multiple linear regressions. The selected reference stations were stations 1 and 2 for station 4 ($0.53 < r < 0.72$; $n = 17$) and stations 1 and 2 for station 5 ($0.59 < r < 0.75$; $n = 16$).

When compared to WXGEN, the statistical correlation method provides better results in reconstructing mean monthly and annual precipitation totals over the documented periods (Table 3). Using multiple regressions applied month-by-month *versus* year-by-year yielded higher monthly correlations for stations 4 (from $r = 0.56$ in winter to $r = 0.62$ in summer) and 5 (from $r = 0.57$ in winter to $r = 0.64$ in summer). Classical percentiles are calculated to evaluate the performance of both WXGEN and the statistical correlation method in reproducing daily precipitation distributions (Table 4). Good agreements between observed and reconstructed daily precipitation data are observed below the 75th percentile for most of the stations using both methods. Some discrepancies appear for the 95th percentile because of extreme precipitation events. The results show a better reproduction of precipitation inter-annual variability with the statistical correlation method. Such statistical characteristics in reconstructed precipitation data are expected for the present study and the daily precipitation dataset generated with the statistical correlation method is therefore selected for further model input.

3.3. Precipitation and river discharge variability

Based on the Tucuman long-term time series ($P_{station5} = 1061$ mm/yr), the annual precipitation over the 1931–1972 period remains below the average over the 1973–2004 period ($P_{1931–1972} = 946$ mm/yr *versus* $P_{1973–2004} = 1175$ mm/yr) even though two short positive periods are observed (i.e. 1957–1960 and 1967–1969; Fig. 2a). Similarly, the annual discharge index shows a negative cycle from the early 1930s to the middle 1970s ($Q_{1931–1972} = 94$ m^3/s *versus* $Q_{1973–2004} = 150$ m^3/s), with a short positive period between 1957 and 1960 (Fig. 2c). Starting in 1973, two contrasting precipitation regimes are apparent with the annual precipitation index estimated from the five stations (Fig. 2b). The first 12 years are characterized by high precipitation totals ($P_{1973–1985} = 1205$ mm/yr) while the nine following years display drier conditions ($P_{1986–1995} = 796$ mm/yr). This climatic trend coincides with hydrological features, such as the annual discharge index, which showed alternating positive ($Q_{1973–1985} = 172$ m^3/s) and negative ($Q_{1986–1995} = 118$ m^3/s) cycles over the 1973–2004 period (Fig. 2c). However, while large temporal trends coincide, the short positive cycle from 1990 to 1993 in the annual discharge index does not match the annual precipitation index (Fig. 2b) for that time period. This discrepancy can be explained by the fact that stations 1 and 4 do not capture extreme precipitation events between 1990 and 1993. It is likely that there is a bias in the estimation of the annual precipitation index by these two stations over 1990–1993, with an under-representation of local climatic trends.

Table 2
The name, location and main characteristics of the gauging station (bracket values refer to the standard deviation of discharge).

	Gauging station	Record period	Latitude (S)	Longitude (W)	Catchment area (km^2)	Average value (m^3/s)	Specific discharge (mm/year)	Proportion of monthly missing data (%)
R3 (Rio Sali-Dulce)	Hondo	1931–2004	27°30′	64°52′	23,334	120 (140)	162 (78)	0

Table 3
Observed and reconstructed mean monthly and annual precipitation totals (mm) using statistical correlation methods and WXGEN over 1973–2004. Note that station 2 has continuous precipitation data except in December 2004.

	Station 1			Station 3			Station 4			Station 5		
	Observed	Reconstructed		Observed	Reconstructed		Observed	Reconstructed		Observed	Reconstructed	
		Statistical correlation	WXGEN		Statistical correlation	WXGEN		Statistical correlation	WXGEN		Statistical correlation	WXGEN
January	358	354	323	104	102	85	134	154	68	181	171	170
February	257	255	265	63	62	66	73	67	105	155	146	129
March	254	253	223	73	73	65	74	85	12	128	122	137
April	131	132	111	16	16	21	24	23	0	82	60	81
May	47	48	58	4	3	11	16	15	17	36	37	25
June	26	27	42	2	2	10	8	7	8	12	12	14
July	17	18	30	1	1	6	12	5	19	21	11	0
August	18	19	28	0	0	8	13	7	18	27	15	17
September	33	29	38	6	6	7	34	35	5	43	44	17
October	86	85	46	27	18	37	43	42	38	101	95	56
November	133	133	135	30	31	31	55	50	38	109	101	108
December	241	245	134	71	71	66	74	67	70	210	214	192
Annual total	1601	1598	1433	397	385	413	560	557	398	1105	1027	946

Table 4
Quantiles for observed and reconstructed daily precipitation using statistical correlation methods and WXGEN over 1973–2004. Note that station 2 has continuous precipitation data except in December 2004.

	Quantiles			
	25%	50%	75%	95%
Station 1				
Observed	3	8	20	62
Statistical correlation	4	8	20	57
WXGEN	4	8	12	49
Station 3				
Observed	5	11	25	60
Statistical correlation	5	10	20	57
WXGEN	4	7	16	50
Station 4				
Observed	1	4	10	40
Statistical correlation	1	4	9	37
WXGEN	0.1	3	6	32
Station 5				
Observed	1	4	10	52
Statistical correlation	1	4	13	55
WXGEN	1	3	12	56

4. SWAT description and implementation

4.1. The SWAT model

SWAT is a physically-based semi-distributed model that operates at the daily time step (Arnold et al., 1998; Neitsch et al., 2002). The spatial variability of land use, soil types and management practices are accounted for by dividing the watershed into multiple Hydrologic Response Units (HRUs) that represent a unique combination of land cover, soil and slope. The climate variables required for running SWAT are daily precipitation along with maximum and minimum air temperatures. In this study, the ArcSWAT 2.1.6 Interface for SWAT2005 was used and hydrological processes were considered only.

The watershed hydrology in SWAT is simulated in two phases. The first phase is the land phase of the hydrologic cycle which calculates the water balance of each HRU in order to provide the amount of water available for the main channel of each sub-basin at a given time step. The second phase is the routing phase which determines the movement of water through the river network towards the basin outlet (Neitsch et al., 2002). The HRU water balance is expressed as follows,

$$W_t = W_o + \sum_{i=1}^{t}(P_i - Q_{isurf} - ET_i - W_{iseep} - Q_{ilat}) \quad (3)$$

where W_t is the soil moisture content at the time t; W_o is the initial soil moisture content; P_i is the amount of precipitation on day i; Q_{isurf} is the amount of surface runoff on day i; ET_i is the amount of evapotranspiration on day i; w_{iseep} is the amount of percolated water through the soil profile on day i; and Q_{ilat} is the amount of groundwater flow on day i. All terms are expressed in mm of water. In SWAT, water that is not removed from the soil by plant uptake or by evaporation can percolate from the bottom of the soil profile through each soil layer into the aquifer, depending on the soils hydraulic conductivity (w_{seep}). Lateral subsurface flow (Q_{lat}) is calculated simultaneously with percolation using a kinematic storage routing method and occurs when the storage in any layer exceeds the field capacity after percolation. Groundwater flow contribution to total streamflow (Q_{gw}) is calculated if the amount of water stored in the shallow aquifer (feed by w_{seep}) exceeds a threshold value.

SWAT provides two approaches for estimating the portion of precipitation that contributes to either surface runoff (Q_{surf}) or

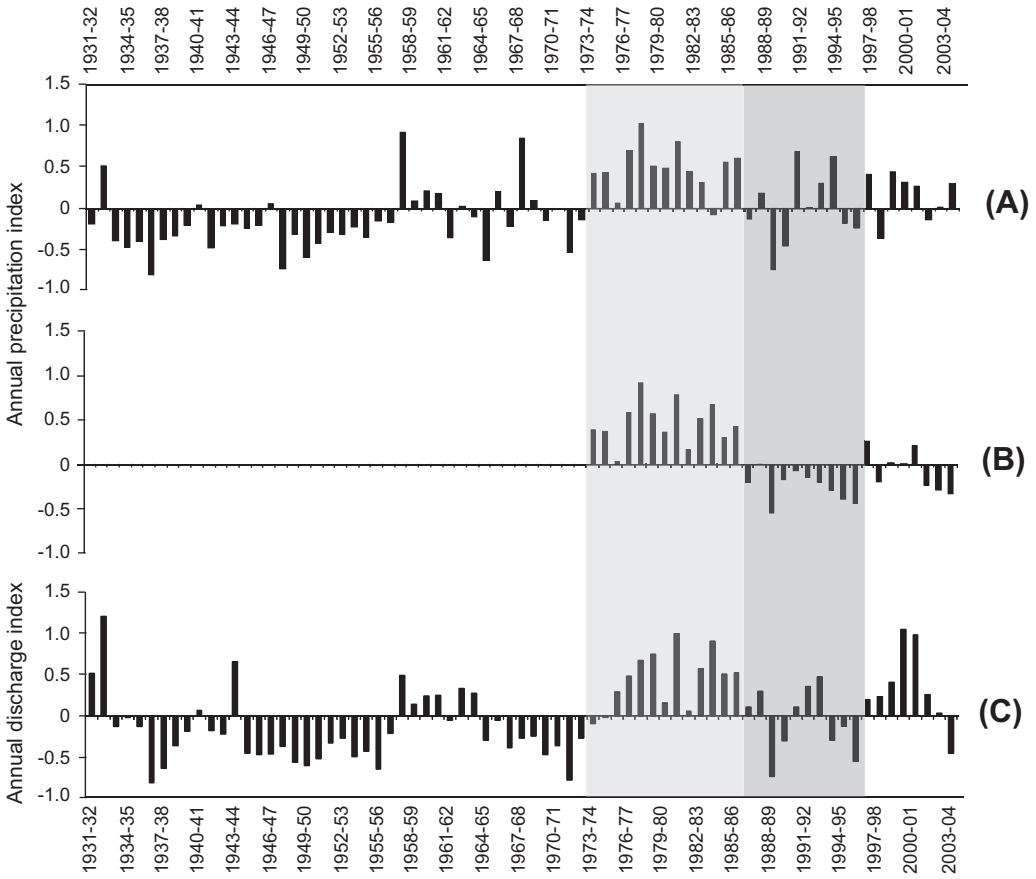

Fig. 2. Annual normalized indexes (I_i) of precipitation obtained from (A) the station 5 over 1931–2004, (B) the five meteorological stations over 1973–2004 and (C) discharge over 1931–2004. I_i is estimated using normal standardization formula as $I_i = (X_i - \overline{X})/\overline{X}$) with X_i and $\overline{X}$ the total and mean annual values respectively (precipitation or discharge). Annual values are calculated for hydrological years (November–October).

infiltration: the SCS curve number procedure (SCS, 1972) and the infiltration method of Green and Ampt (1911). The infiltration method is physically-based but requires input data at a finer-than-daily time resolution. We have chosen the empirical SCS approach which is based on more than 20 years of studies involving rainfall–runoff relationships from watersheds across the United States and requires daily precipitation data only. Of the three methods available in SWAT for calculating potential evapotranspiration (PET), we selected the Hargreaves method (Hargreaves and Samani, 1985), a robust approach (Heuvelmans et al., 2005) requiring daily temperature only.

Model performance is evaluated at the monthly time step using the Nash–Sutcliffe efficiency (*NSE*; Nash and Sutcliffe, 1970) given by

$$NS = 1 - \left[\frac{\sum_{i=1}^{N}(O_i - S_i)^2}{\sum_{i=1}^{N}(O_i - \overline{O})^2}\right] \quad (4)$$

where O_i refers to the observed streamflow for month i, $\overline{O}$ is the mean monthly observed streamflow and S_i is simulated streamflow for month i. *NSE* is a normalized statistic that determines the relative magnitude of the residual variance compared to the observed data variance and ranges between $-\infty$ and 1, with *NSE* = 1 being the optimal value. Moriasi et al. (2007) specified the following criteria for interpreting model performance at the monthly time scale: *NSE* values greater than 0.75 are considered "very good", values between 0.75–0.65 and 0.65–0.50 are considered "good" and "satisfactory" respectively and values below 0.50 are considered "unsatisfactory".

4.2. Spatial database and HRU delineation

A 90-m resolution topography obtained from the Shuttle Radar Topography Mission (SRTM DEM) was used as the basis for modeling processes (Fig. 1). The main channel was created from the DEM by the ArcSWAT interface using a threshold drainage unit area of 10^8 m^2 and 31 sub-basins were obtained. The land cover classification at a 300-m spatial resolution was obtained from GlobCover version 2 established between 2004 and 2006. The land cover types consist of cropland (44.53%), forests (deciduous and evergreen; 34.32%), shrublands and grasslands (19.85%), water bodies (1.12%), urban zones (0.14%) and wetlands (0.04%). The regional SOTER soils map for South America and a database at 1/5,000,000 scale (SOTWIS-World Soils and Terrain Digital Databases) supplied soils information (Nachtergaele et al., 2009). Five soil types were identified in the basin: Lithic Leptosols (LPq), Luvic Phaeozems (PHl), Eutric Regosols (RGe), Calcaric Regosols (RGc) and Eutric Fluvisols (FLe). The 31 sub-basins were subdivided into 120 hydrological response units (HRUs) assuming threshold levels of 20%, 10% and 20%, respectively, that represent the dominant land cover, soil types, and slope characteristics.

4.3. Water impoundment and management practices within the basin

Reservoirs play an important role in water supply and flood control by reducing peak flow and supporting low flow. In SWAT, the recommended method for calculating large reservoir outflow is the target release approach which estimates water flow as a function of the desired target storage. This approach tries to mimic

Table 5
Characteristics and input variables for the Rio Hondo reservoir. *Source*: Laboratorio de Hidráulica at the Universidad Nacional de Córdoba.

Input variables	Definition	Value
RES_ESA	Surface area of the reservoir when filled to the emergency spillway (ha)	33,000
RES_PSA	Surface area of the reservoir when filled to the principal spillway (ha)	31,000
RES_EVOL	Volume of water needed to fill the reservoir the emergency spillway (m^3)	$127{,}000 \times 10^4$
RES_PVOL	Volume of water needed to fill the reservoir to the principal spillway (m^3)	$110{,}000 \times 10^4$
RES_VOL	Volume of water needed to fill the reservoir to the principal spillway (m^3)	$110{,}000 \times 10^4$
RES_K	Effective saturated hydraulic conductivity of the reservoir bottom (mm/h)	0[a]
IRESCO	Outflow method	Simulated target release
RES_RR	Average daily principal spillway release rate (m^3/s)	10
IFLOD1R	Beginning month of the flood season	November
IFLOD2R	Ending month of the flood season	June
NDTARGR	Number of days required for the reservoir to reach target storage	10

[a] The hydraulic conductivity is set to zero since no seepage is assumed to occur.

general release rules that may be used by reservoir operators and is able to simulate major outflow and low flow periods. The principal spillway volume corresponds to the maximum flood control reservation while the emergency spillway volume corresponds to the no flood control reservation. Characteristics and input variables are listed in Table 5.

We account for the water removed in the Sali-Dulce Basin to meet water consumption needs. We set water use in urban zones as equal to 341 L/day per inhabitant (http://www.canoa.org.ar/) and calculated the average daily water removal within each reach (i.e., on average from 2 to 28×10^4 m^3) in sub-basins where the main urban zones are located. In the present study, there is no consideration of changes in consumptive water use.

5. Results and discussion

5.1. Model calibration and validation

5.1.1. Cross calibration strategy

The calibration period covers the precipitation trends observed from 1973 to 2004. As described in Section 3.3, this time interval includes two time-equivalent periods with contrasted climatic conditions, referred to as the wet (A: 1976–1985) and dry (B: 1986–1995) periods. Both periods are used for the cross-calibration strategy. The implemented three-step cross-calibration exercise consists in: (1) conducting a sensitivity analysis to identify the sensitive hydrological parameters over each calibration period (A and B) and for a period reconciling both climatic conditions (A + B: 1976–1995), (2) adjusting the values for the selected sensitive parameters and (3) validating the A and B parameter sets on the opposite climatic period. The 1996–2004 period is used as a common validation period for the three parameter sets. All the 28 parameters describing the hydrological cycle were included in the sensitive analysis performed with the LH-OAT method (Latin Hypercube One-factor-At-a-Time: van Griensven et al., 2006). Details for all of the SWAT's hydrological parameters can be found in Winchell et al. (2007). The most sensitive parameters were adjusted using the autocalibration procedure included in SWAT (Parameter Solutions Method; PARASOL; van Griensven et al., 2002).

Table 6 gives the rank of the seven most sensitive parameters as determined from the LH-OAT method for each calibration period. The seven selected parameters were adjusted for each calibration period using the autocalibration procedure included in SWAT. The first 3 years of each calibration period equilibrate the model to the basin conditions. The optimal value of each parameter is presented in Table 6.

5.1.2. SWAT simulation results

The model simulates the monthly mean discharge with an acceptable accuracy over the wet and dry climatic conditions with a low decrease in model performance between the calibration and validation periods (Table 7). The lower SWAT performance in simulating streamflow over the wet calibration period might result from the higher proportion of missing precipitation data. However, the monthly discharges are simulated in an acceptable way over the wet period for both the calibration (NSE_{wet} = 0.86) and validation (NSE_{wet} = 0.84), underlying the relevance of the statistical correlation methods for filling data gaps. The average magnitude of simulated discharges between the calibration and validation periods is maintained below 10% (i.e. low model bias) over the wet and dry periods showing the robustness of SWAT throughout the contrasted climatic conditions.

Nevertheless, the highest model performance is observed for the entire calibration period covering mixed climatic conditions (NSE_{A+B} = 0.91) with a better peak flow (NSE = 0.81) and baseflow (NSE = 0.74) prediction (Fig. 3), and a more realistic total volume simulation (Q_s/Q_o). The A + B calibrated parameters is therefore considered as being the most appropriate set for a long-term simulation and selected for the following analyses.

Table 6
Rank of the seven most sensitive parameters, their range and their fitted value.

Group	Parameter	Description	Period A	Period B	Period A + B	Range	Default value	Period A	Period B	Period A + B
Infiltration	CN2	Initial SCS CN2 value	1	1	1	±25%	Soil data	−14.0	−13.8	−13.2
Evaporation	ESCO	Soil evaporation compensation factor	2	2	2	0–1	0.95	0.5	0.7	0.6
Groundwater	GWQMN	Threshold water depth in shallow aquifer for baseflow to occur	3	3	3	0–1000 mm	0	990	686	890
Surface runoff	SURLAG	Surface runoff lag coefficient	4	4	7	1–24 days	4	5	10	8
Interception	CANMX	Maximum canopy stockage	5	7	4	0–10 mm	0	8.3	8.9	8.8
Crop	BLAI	Potential maximum leaf area index for crops	6	6	5	0–1	Soil data	0.92	0.98	0.75
Soil	SOL_AWC	Available water capacity	7	5	6	±25%	Soil data	24.9	24.7	24.8

Table 7
Model performance during the calibration and validation periods. Note that the values for each evaluated period take into consideration the initialisation years.

Calibration period	Evaluated period	NSE discharge	NSE peak flow*	NSE baseflow**	Q_s/Q_o
A	Wet calibration: 1979–1985	0.86	0.72	0.64	1.10
A	Dry validation: 1989–1995	0.78	0.62	0.57	1.13
A	Common validation: 1996–2004	0.61	0.37	0.30	1.15
B	Dry calibration: 1989–1995	0.90	0.70	0.73	1.06
B	Wet validation: 1979–1985	0.84	0.61	0.70	1.09
B	Common validation: 1996–2004	0.63	0.40	0.42	1.08
A + B	Mixed calibration: 1979–1995	0.91	0.81	0.74	1.05
A + B	Common validation: 1996–2004	0.64	0.53	0.43	1.06
A + B	Observed data conditions (*M1*): 1934–1972	0.61	0.59	0.51	0.82
A + B	Generated data conditions (*M2*): 1934–1972	0.71	0.69	0.59	0.89

* Estimated during the high-flow period from January to March.
** Estimated during the low-flow period from August to October.

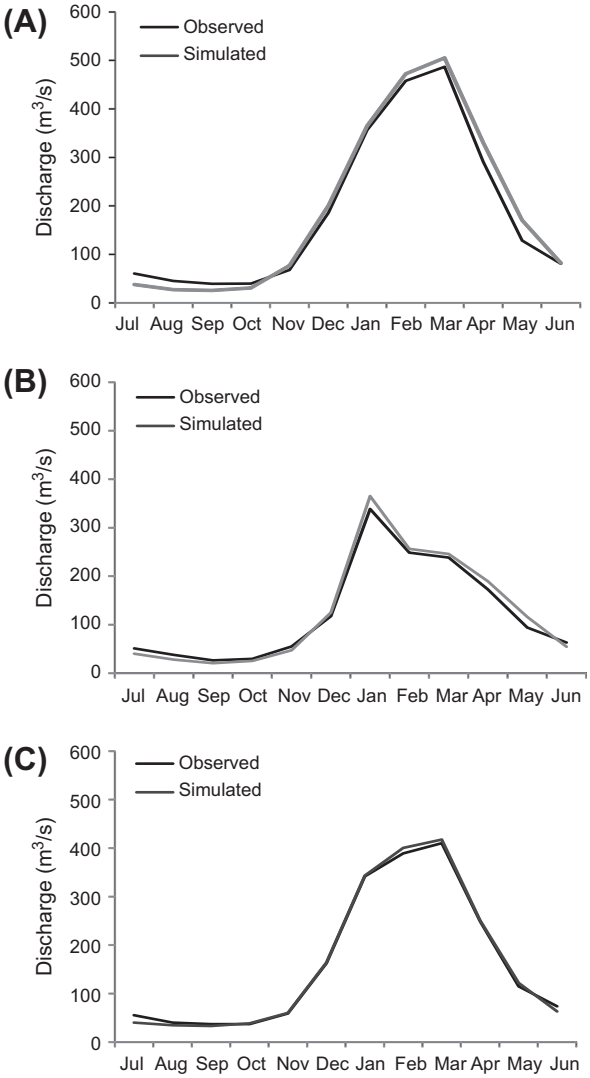

Fig. 3. Observed (bold black line) and simulated (gray line) monthly mean discharges over the calibration period for the calibrated parameter sets during the (A) period A, (B) period B, and (C) period A + B.

The results over the 1996–2004 common validation periods show a decrease in model performance compared to the performance over the calibration periods (Fig. 4 and Table 7). This could be related to errors in the observed discharge data or to an unusual functioning of the Rio Hondo reservoir. The latter explanation is the most likely since SWAT adequately predicts the amount of water flowing from the Rio Hondo reservoir (as suggested by the Q_s/Q_o values in Table 7) despite simulating abnormal seasonal discharge patterns. Unfortunately, the lack of information on the recent worsening of environmental problems in the Rio Hondo reservoir (e.g. sediment filling, eutrophication, etc.) makes the evaluation of this assumption difficult.

5.2. Model adaptation to changing climatic conditions

The analysis of the physical meaning of the calibrated parameter sets (Table 6) illustrates the way the model adapts its structure to climatic conditions. The most sensitive parameter is the runoff coefficient (CN2), obtained by calculating the amount of surface runoff following a precipitation event. Although the SCS curve number method is empirically-based, the stability of CN2 values over the three calibration periods (ΔCN2 < 1%) indicates the robustness of the SCS method under varying climatic conditions. The second dominant parameter is related to soil moisture depletion by evaporation. The lower ESCO value for period B means that SWAT extracts more water for evaporation from deeper levels over the dry period. The groundwater parameter related to the threshold water depth in the shallow aquifer for baseflow to occur ranked next. The lower GWQMN value for period B indicates significant exchanges between the shallow aquifer and the stream over the dry period. SURLAG regulates the delay in release of surface runoff in the stream. Large basins with a residence time greater than 1 day are particularly sensitive to SURLAG since only a portion of the surface runoff will reach the main channel on the day it is generated. The highest SURLAG value for period B reflects smoother streamflow hydrographs over the dry period. CANMX is related to interception and defines the maximum amount of water trapped in the canopy. The lower CANMX value for period A indicates a weakening of the interception process during high precipitation events. BLAI controls the leaf area development of a plant during the growing season. Its sensitivity is not surprising since cropland and forests are the main land cover types in the Sali-Dulce Basin. However, the lower value for the combined A + B period than for the individual A and B periods makes its physical interpretation difficult. The last most sensitive parameter is related to available water capacity (SOL_AWC). The adjusted values are similar over the three calibration periods and higher (i.e. 25%) than default values in the soil database.

Table 8 summarizes the main components of the simulated water balance over the wet and dry periods for the Sali-Dulce Basin. Compared to the wet period, the runoff ratio (Q/P) is lower over the dry period. This indicates that the reduction in river discharge is proportionally higher than the precipitation decrease. The basin's groundwater ratio, which defines the interaction between groundwater and streamflow, shows a higher groundwater contribution to surface runoff over the dry period. The baseflow

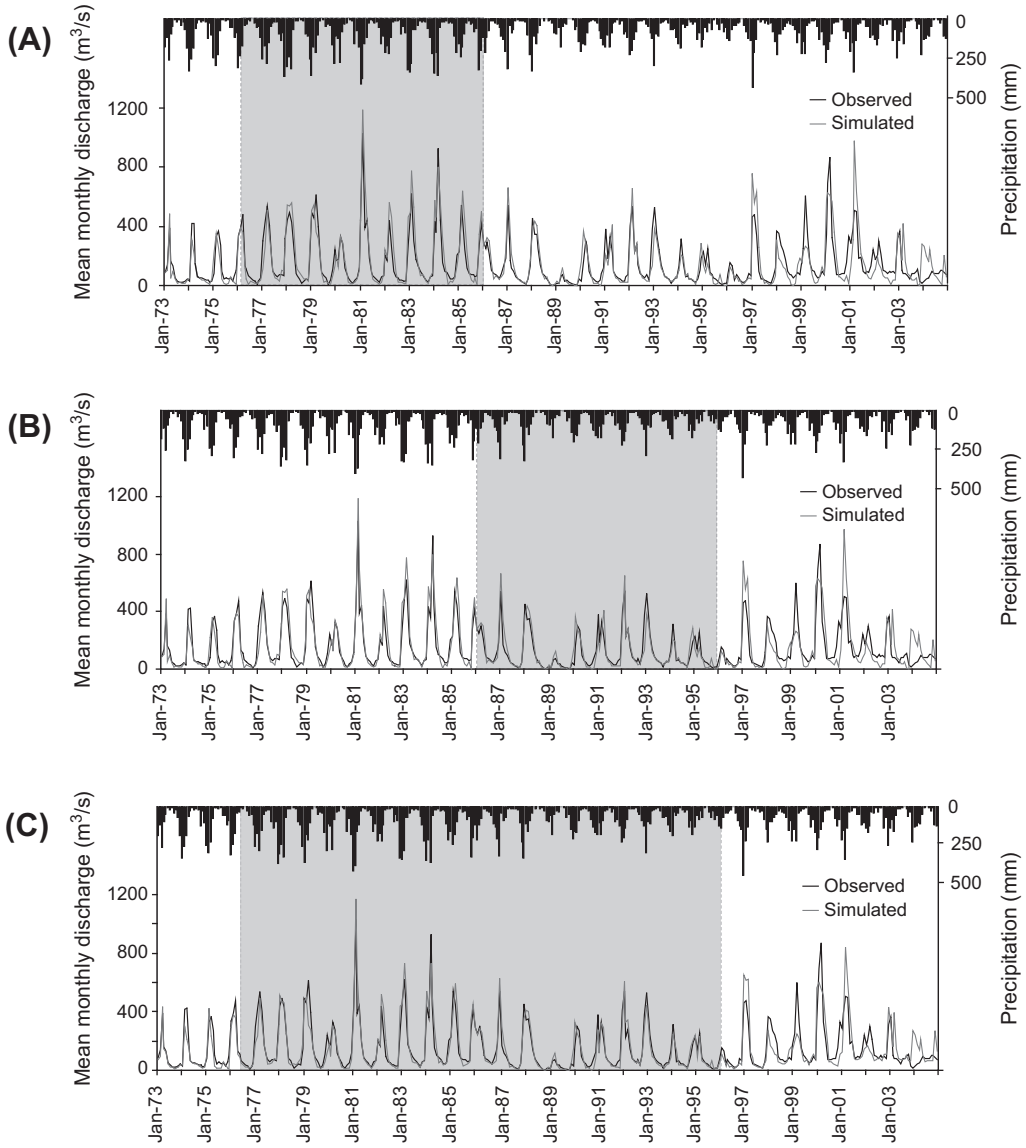

Fig. 4. Observed (bold black line) and simulated (gray line) monthly discharges with respect to the precipitation depth over the calibration (gray rectangle) and validation periods for the calibrated parameter sets during the (A) period A, (B) period B, and (C) period A + B.

Table 8
Simulated annual water balance components using parameter sets calibrated for mixed (A + B) climatic conditions over the wet and dry periods with P, rainfall; ET_a actual evapotranspiration; Q_o and Q_s observed and simulated surface runoff, respectively; Q_{gw} simulated groundwater flow; PERC water percolating from the shallow aquifer into the deep aquifer; Q_s/P the basin's runoff ratio; Q_{gw}/Q_s the basin's groundwater ratio; and SW, soil moisture content. All terms are expressed in mm. Note that the values for each evaluated period take into consideration the initialisation years.

Evaluated period	P	ET_a	Q_o	Q_s	Q_{gw}	PERC	Q_s/P	Q_{gw}/Q_s	SW
Wet: 1979–1985	1205	752	265	290	55	163	0.241	0.19	425
Dry: 1989–1995	796	631	150	161	53	4	0.202	0.33	352

contribution to streamflow in the reach remains constant over the wet and dry periods. The deep percolation is drastically reduced over the dry period meaning that aquifers in the Sali-Dulce Basin are no longer recharged during dry periods.

5.3. SWAT simulation under scarce data conditions

The estimation of rainfall over the watershed area is one of the most important aspects that determine the performance of a river discharge simulation. Over the 1931–1972 period, only two meteorological stations are available for the Sali-Dulce Basin (Table 1 and Fig. 1). Given such limited input data, a satisfactory model performance is not expected. We therefore proposed a long-term simulation based on two different ways of using available precipitation data. The first method ($M1$) is to directly introduce the two precipitation time series (stations 5 and 6) and let SWAT determine the spatial distribution of the precipitation (each subbasin is assigned to the nearest station). The drawback of this method is to add a meteorological station not used in the initial calibration procedure. The second strategy ($M2$) is to mimic the

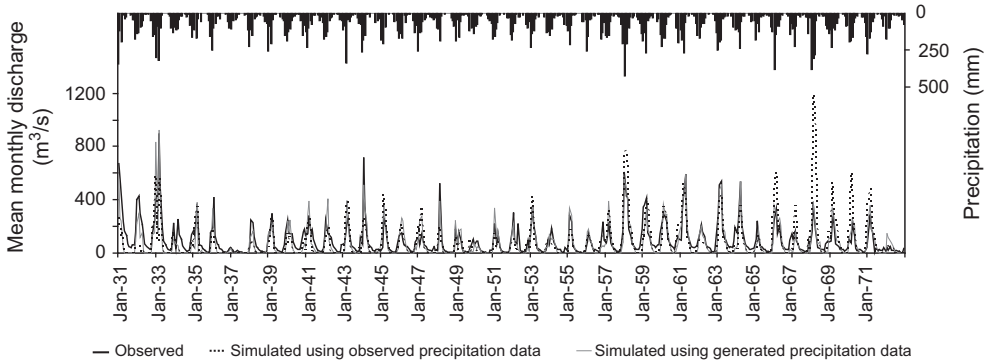

Fig. 5. Observed (black line) and simulated monthly discharges in conditions of observed (dotted black line) and generated (gray line) precipitation data with respect to the precipitation depth over 1931–1972.

spatial distribution of the precipitation that resulted from the calibration procedure by reproducing the network of the five meteorological stations. To do so, the normal ratio method, based on monthly ratios calculated over the 1973–2004 period, is used (see Section 3.2). Station 5 is used to extend the daily precipitation period back to 1931. The model is run using the A + B calibrated parameters.

The estimated amount of precipitation by SWAT is higher with the *M*1 (P = 577 mm/yr) than the *M*2 method (P = 404 mm/yr) and differences in model performances are observed (Table 7 and Fig. 5). The highest model efficiency in reproducing surface runoff, peak flow and baseflow is provided by the SWAT simulation performed with generated precipitation data (Table 7). Both methods underestimate total volumes over the 1931–1972 period compared to the ones obtained over the calibration and validation periods. This might be caused by an underestimation of areal precipitation or a change in the basin conditions. Nevertheless, the evaluation of these assumptions remains difficult given the scarce data availability.

5.4. Scenario simulations

In this study, simulations under different scenario conditions are performed in order to analyze the impacts of climate and land cover changes on streamflow sensitivities. One of the main interests is to provide a better understanding of the increase in discharge observed in the 1970s in the Sali-Dulce Basin.

5.4.1. Streamflow sensitivities to climate changes

Climatic scenarios are performed to assess the respective impact of precipitation and temperature changes on streamflow. The three predefined periods representing the wet (1976–1985), dry (1986–1995) and mixed (1976–1995) climatic periods are used as baseline conditions. We examined a 1–2 °C change in daily temperature (Fig. 6a) and 10–20% change in daily precipitation (Fig. 6b).

As temperature increases (decreases) by 2 °C, streamflow decreases (increases) by 9% (11%) compared to the mixed baseline values with a variation of 5–12% (8–15%) between dry and wet baseline periods respectively. A stronger temperature impact is observed when the model starts from the wet situation. The impacts of temperature on streamflow are due to its effects on evapotranspiration. These results highlight the forcing factors that impact actual evapotranspiration: actual evapotranspiration is less climate-dependant and more water-dependent when water availability decreases.

Streamflow is found to be very sensitive to the prescribed precipitation changes. When compared to the mixed baseline values, a

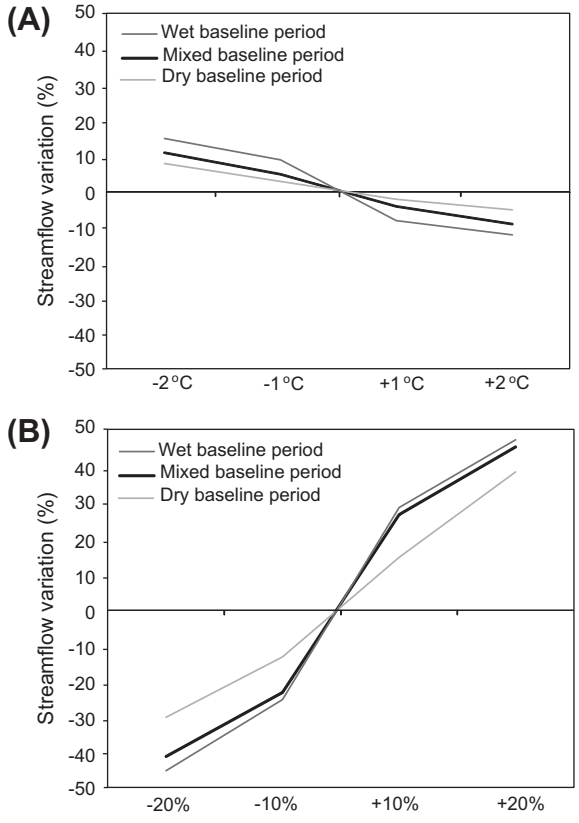

Fig. 6. Streamflow variation in response to changes in (A) temperature and (B) precipitation under wet (dark gray line), mixed (black line) and dry (gray line) baseline periods.

20% increase (decrease) in precipitation results in an increase (decrease) by 46% (41%) in streamflow, a variation of 39–48% (30–45%) over the dry and wet baseline values respectively. In order to illustrate the non-linearity of the response in streamflow to variations in precipitation, the precipitation elasticity (ε_p) of streamflow is calculated using the formulation proposed by Sankarasubramanian et al. (2001) as follows:

$$\varepsilon p = \frac{dQ/\overline{Q}}{dP/\overline{P}} \tag{5}$$

Its value is higher for a 10% precipitation increase compared to one of 20%, starting from the mixed ($\varepsilon_{p10\%}$ = 2.7 *versus* $\varepsilon_{p20\%}$ = 2.3) and wet ($\varepsilon_{p10\%}$ = 2.9 *versus* $\varepsilon_{p20\%}$ = 2.4) baseline periods. In contrast,

starting from the dry baseline values, the precipitation elasticity of streamflow increases as precipitation increases from 10% to 20% ($\varepsilon_{p10\%} = 1.5$ *versus* $\varepsilon_{p20\%} = 2.0$). Similar results are seen with a decrease in precipitation. A small change in precipitation seems to have larger impacts on streamflow over the mixed and wet periods. The decrease in precipitation elasticity between wet and dry baseline conditions implies that when the catchment is wetter, the buffering effect of soil retention decreases and precipitation excess promotes runoff generation.

5.4.2. Streamflow sensitivities to land cover changes

Northern Argentina has encountered an important expansion of cultivated areas over the last quarter of the 20th century, largely due to the soybean boom in Argentina (De Lima, 2001; Barros, 2004). Two scenarios of land cover change are evaluated to determine their potential contribution to the significant increase in discharge of the 1970s in the Sali-Dulce Basin. The first scenario assumes a decrease in cultivated areas compared to the present condition. The main category of cropland representing 23.56% of the catchment area is replaced in favor of rangeland; the corresponding change is a decrease in cultivated areas by 53%. The second scenario assumes an increase in cultivated areas compared to the present situation. Two classes of rangeland (shrubland and grassland) representing 19.38% of the catchment area are converted into cropland; the corresponding change is an increase in cultivated areas by 44%. SWAT is then run over the 1976–1995 period with the A + B calibrated parameters. The first scenario produces a 12.5% decrease in mean monthly streamflow with respect to the reference value, while the second scenario leads to a 13% increase in mean monthly streamflow with respect to the reference value. The streamflow changes are compensated by changes in actual evapotranspiration values (±9%), which are linked to variations in the water retention capacity of cultivated areas. It also showed that changes in water consumption (±40%) lead to relatively low streamflow variations (<8%) that seem to offset the impacts of the expansion of cultivated areas.

5.4.3. Insights into the driving factors of the 1970s hydrological changes

It is of regional interest to investigate the factors responsible for the increase in discharge of the 1970s since the abrupt lake level rise of Laguna Mar Chiquita also coincided significantly with the Rio Sali-Dulce discharge trends. Consequently, the impact of the observed precipitation change between 1931–1972 and 1973–2004 ($\Delta P/\overline{P} = +22\%$; see Section 3.3) on the streamflow of the Rio Sali-Dulce is evaluated starting from the 1931–1972 and 1986–1995 dry baseline periods.

The simulated mean streamflow is increased by 42% and 44% over the 1931–1972 and 1986–1995 periods respectively. The predicted streamflow changes are in close agreement with the observed changes ($\Delta Q/\overline{Q} = 45\%$). However, uncertainties from the estimated changes in precipitation, linked to the fact that only one meteorological station was only available, raise doubts about the accuracy of the simulated streamflow changes (Table 1). We believe that the 1970s precipitation increase estimated at 22% is over evaluated since streamflow is under- and over-estimated prior and after 1972 respectively (see Section 5.3). Taking into account the uncertainties in the simulated discharges, our results suggest that, while the extension of cultivated areas likely contributed to the 1970s streamflow increase in the Sali-Dulce Basin, changes in precipitation remain the dominant driving factor.

6. Towards a hydrological basin-lake model

One important goal of this study was to provide an integrated basin-lake model able to reproduce the hydrological trends of Laguna Mar Chiquita levels over the 1970s hydroclimatic transition period in central Argentina. As mentioned, streamflow in the Sali-Dulce Basin was shown to be the main driver of the abrupt increase in the 1970s level observed in Laguna Mar Chiquita given that 92% of the lake level rise was attributed to an increase in the Rio Sali-Dulce discharge (Troin et al., 2010). Obtaining a basin-lake model is achieved by integrating the SWAT simulation of the Rio Sali-Dulce discharge (Q_{R3}) performed with the A + B calibrated parameters into the lake model. The dynamic lake water balance equation at the monthly time scale Δt is given by

$$\frac{\Delta V}{\Delta t} = A(V)(P - E) + Q_{in} - \gamma \tag{6}$$

with

$$Q_{in} = Q_{R1} + Q_{R2} + Q_{R3} \tag{7}$$

where ΔV is the lake volume variation (m^3); A is the lake area (m^2) as a function of lake volume V; P is on-lake precipitation (m) estimated from six rainfall stations located around the lake (Fig. 1); E is the evaporation from the lake surface (m) calculated using the Complementary Relationship Lake Evaporation (CRLE) Model (Morton, 1983; DosReis and Dias, 1998); Q_{in} is the water inflow from the catchment (m^3); Q_{R1} and Q_{R2} are the two southern river discharges; Q_{R3} is the Rio Sali-Dulce discharge corresponding to 90% of Q_{in}; and the γ parameter refers to the water loss by evapotranspiration in un-gauged surfaces representing 80% of the lake catchment. Its constant value reflects the fact that un-gauged surfaces are not climate-dependant as discussed in Troin et al. (2010). The corresponding lake level is estimated as a function of lake volume, $h = f(V)$, following the morphometric relationship established using lake bathymetry (Hillman, 2003).

Lake level simulations are first performed over the 1973–2004 period using the observed and simulated Rio Sali-Dulce discharges (Q_{R3}). Lake level variations are well reproduced using the simulated discharge (Fig. 7) with a model efficiency ($NSE = 0.91$) similar to the performance using the observed Rio Sali-Dulce discharge

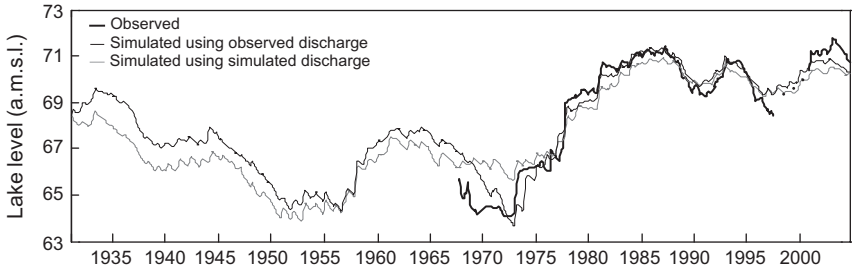

Fig. 7. Observed (bold line) and simulated lake levels of Laguna Mar Chiquita over 1931–2004 using observed (black line) and simulated (gray line) Rio Sali-Dulce discharges. Observed lake levels are continuous since 1967 except a gap between 1997 and 2001 where only three monthly measurements of water level are available.

(*NSE* = 0.93; Troin et al., 2010). Over 1931–2004, the SWAT simulation from generated precipitation data provides lake level trends that are synchronous with those proposed by Troin et al. (2010). However, the low lake level observed in the late 1960s until the early 1970s is not well captured by the basin-lake model (Fig. 7). One reason for such poor performance might come from the inadequate representation of watershed area rainfall from 1966 to 1971. Station 5, selected to extend the daily precipitation data of the stations 1, 2, 3 and 4 (see Section 5.3) back to 1931, shows records of extreme precipitation events ($\Delta P_{1966-1971}$ = +16%), specifically with a wetter year in 1968 (ΔP = +72%). It is likely that extreme events create a bias in the estimation of the watershed area rainfall over the 1966–1971 period with an over representation of local climatic influence. Reasonable simulations of the long-term lake level tendencies are therefore observed despite the propagation of uncertainties in simulating streamflow in the Sali-Dulce Basin. The basin-lake model allows an adequate reproduction of the key hydrological trends in Laguna Mar Chiquita with low lake levels during the entire first three-quarters of the 20th century interrupted by two moderately high lake levels centered approximately around 1935 and 1960, followed by the 1970s rise and high stands in the 1980s, 1990s and 2000s.

7. Conclusions

In this study, attempts are made to propose an integrated basin-lake model able to reproduce the 1970s hydrological changes observed in the Laguna Mar Chiquita catchment in central Argentina. Since the abrupt rise of Laguna Mar Chiquita levels in the 1970s was shown to be driven by an increase in the Rio Sali-Dulce discharge, the main objective was to use the physically-based SWAT model to simulate streamflow in the Sali-Dulce Basin in order to decipher the respective roles of climate and land cover change on the regional hydrological changes.

In Argentina, the meteorological station network is not very dense; duration time series are quite short and include many missing data. The primary focus of this study was to select the relevant method to fill gaps in daily precipitation data. Aside from the WXGEN weather generator included in SWAT, alternative methods such as a statistical correlation method are examined. Our analyses of daily precipitation distributions indicate a better reproduction of the inter-annual variability precipitation with the statistical correlation method and the resulting generated daily precipitation datasets are selected as model inputs.

Secondly, the ability of SWAT to simulate non-stationary hydrological conditions is evaluated by a cross-calibration experiment. Based on observed daily meteorological data over 1973–2004, two successive 9-year periods referred to as wet and dry periods are selected. The calibration results in similar model efficiencies at the monthly time scale over the wet and dry periods. The model validation on the opposite climatic periods indicates a low magnitude of simulated discharges (i.e. low model biases) demonstrating SWAT's robustness to adapt its structure to changing climatic situations. The highest model performance in simulating surface runoff, peak flow and baseflow over the 1996–2004 period is therefore reached with a calibration period that combines both wet and dry conditions. An extension of the SWAT simulation back to 1931 based on generated daily precipitation data from statistical correlation methods is proposed.

Different scenario conditions are then developed in order to analyze the impacts of climate and land cover changes on streamflow sensitivities in the Sali-Dulce Basin. When precipitation is increased until it reaches the 1970s precipitation change ($\Delta P/\overline{P} = 22\%$), the resulting streamflow increase closely matches the 1970s hydrological change ($\Delta Q/\overline{Q} = 45\%$). Sensitivity analyses reveal that the extension of cultivated areas only had a minor impact on the 1970s hydrological changes in the Sali-Dulce Basin.

Finally, integrating the SWAT simulation in the lake water balance model over the 1973–2004 period yields lake level variations similar to those obtained with observed discharge values. Over 1931–2004, the general trends in lake level fluctuations are well reproduced except for the low level in the early 1970s. These results suggest that this integrated basin-lake model is a promising approach for simulating long-term lake level variations in response to climate. This modeling approach may be used as a valuable tool for simulating future hydrological responses and for reconstructing past climatic conditions, which will improve our understanding of climate variability in this region of South America.

Acknowledgements

The work presented was supported by a PhD grant from the French Ministry (Magali Troin), and benefited from funding from the French CNRS-INSU (PNEDC and LEFE-EVE programs, AMANCAY Project) and from the French National Research Agency (Program VMC, Project ANR-06-VULN-010, ESCARSEL Project). The work was also part of the CLARIS-LBP Project (EC-FP7), ECOS *Sud*-MINCYT (A08U03, France–Argentina cooperation) and PIP 112-200801-00808 (CONICET). We express our sincere gratitude to Joël Guiot for his suggestions in climate statistics and the SIGéo service at CEREGE for their help in the GIS data construction. We also thank the SWAT user group for exchanging ideas and for discussing issues regarding use of the ArcSWAT interface. The authors would like to thank the anonymous reviewers for their interesting comments and suggestions.

References

Abdo, K.S., Fiseha, B.M., Rientjes, T.H.M., Gieske, A.S.M., Haile, A.T., 2009. Assessment of climate change impacts on the hydrology of Gilgel Abay catchment in Lake Tana basin, Ethiopia. Hydrol. Process. 23, 3661–3669.

Anderson, R.M., Koren, V.I., Reed, S.M., 2006. Using SSURGO data to improve Sacramento Model a priori parameter estimates. J. Hydrol. 320, 103–116.

Apaydin, H., Anli, A.S., Ozturk, A., 2006. The temporal transferability of calibrated parameters of a hydrological model. Ecol. Model. 195, 307–317.

Arnold, J.G., Srinivasan, R., Muttiah, R.S., Williams, J.R., 1998. Large area hydrologic modelling and assessment – part I: model development. J. Am. Water Resour. Assoc. 34 (1), 73–89.

Bardossy, A., Das, T., 2008. Influence of rainfall observation network on model calibration and application. Hydrol. Earth Syst. Sci. 12, 77–89.

Barros, V., 2004. Tendencias climaticas en la Argentina: precipitacion. Proyecto Agenda Ambiental regional-Mejora de la Gobernabilidad para el Desarrollo Sustentable PNUD Arg./03/001. Fundacion torcuato di tella y secretaria de Medio Ambiente y Desarrollo Sustentable.

Beven, K.J., 2004. Rainfall–Runoff Modelling: The Primer. John Wiley and Sons, Chichester, UK.

Bianchi, A.F., Yañez, C.E., 1992. Las precipitaciones en el noroeste Argentino. Segunda Edicion. Instituto nacional de tecnologia agropecuaria estacion experimental agropecuaria Salta.

Borman, H., Breuer, L., Gräff, T., Huisman, J.A., 2007. Analyzing the effects of soil properties changes associated with land use changes on the simulated water balance: a comparison of three hydrological catchment models for scenario analyses. Ecol. Model. 209, 29–40.

Borman, H., 2008. Sensitivity of a soil–vegetation–atmosphere transfer scheme to input data resolution and data classification. J. Hydrol. 351, 154–169.

De Lima, M.A., 2001. Mudancas Climaticas Globais e a Agropecuaria Brasileira, p. 9.

DosReis, R.J., Dias, N.L., 1998. Multi-season lake evaporation: energy-budget estimates and CRLE model assessment with limited meteorological observations. J. Hydrol. 208, 135–147.

Figueroa, L.R., Medina, L.F., Pietroboni, A.M., 1996. Variaciones del nivel freático en la llanura deprimida de Tucuman. INTA-CRTS, Serie Monográfica 3.

Galvan, A.F., 1981. Description geologica de la Hoja 10 a Cafayate, Provincias de Tucuman, Salta y Catamarca.

Garcia, N.O., Vargas, W.M., 1998. The temporal climatic variability in the Rio de la Plata basin displayed by the river discharge. Clim. Change 38 (3), 359–379.

Garcia, N.O., Mechoso, C.R., 2005. Variability in the discharge of South American rivers and in climate. Hydrol. Sci. 50 (3), 459–478.

Garcia, M.G., Sracek, O., Fernandez, D.S., del Valle Hidalgo, M., 2006. Factors affecting arsenic concentration in groundwaters from Northwestern Chaco-Pampean Plain, Argentina. Environ. Geol. http://dx.doi.org/10.1007/s00254-006-0564-y.

Gassman, P.W., Reyes, M.R., Green, C.H., Arnold, J.G., 2007. The soil and water assessment tool: historical development, applications, and future research directions. Trans. Am. Soc. Agric. Biol. Eng. 50, 1211–1250.
Green, W.H., Ampt, G.A., 1911. Studies on soil physics, 1. The flow of air and water through soils. J. Agric. Sci. 4, 11–24.
Hall, A.J., Rebella, C.M., Ghersa, C.M., Culot, J.P., 1992. Field crop systems of the Pampas. In: Peterson, C.J. (Ed.), Field Crop Ecosystems. Elsevier, Amsterdam, pp. 413–450.
Hargreaves, G.H., Samani, Z.A., 1985. Reference crop evapotranspiration from temperature. Appl. Eng. Agric. 1 (2), 96–99.
Hastenrath, S., 1991. Climate Dynamics of the Tropics. Kluwer Academic Publishers, Dortrecht.
Heuvelmans, G., Garcia-Qujano, J.F., Muys, B., Feyen, J., Coppin, P., 2005. Modelling the water balance with SWAT as part of the land use impact evaluation in a life cycle study of CO_2 emission reduction scenarios. Hydrol. Process. 19, 729–748.
Hillman, G., 2003. Analysis y simulacion hidrologica del sistema de Mar Chiquita. Unpublished Thesis, Universidad Nacional el Cordoba, Argentina.
Klemes, V., 1986. Operational testing of hydrological simulation models. Hydrol. Sci. J. 31, 13–24.
Kröhling, D.M., Iriondo, M., 1999. Upper Quaternary palaeoclimates of the Mar Chiquita area, North Pampa, Argentina. Quatern. Int. 57–58, 149–163.
Leavesley, G.H., 1994. Modeling the effects of climate change on water resources – a review. Clim. Change 28, 159–177.
Legesse, D., Vallet-Coulomb, C., Gasse, F., 2003. Hydrological response of a catchment to climate and land use changes in Tropical Africa: case study South Central Ethiopia. J. Hydrol. 275, 67–85.
Legesse, D., Abiye, T.A., Vallet-Coulomb, C., Abate, H., 2010. Streamflow sensitivity to climate and land cover changes: Meki River, Ethiopia. Hydrol. Earth Syst. Sci. 14, 2277–2287.
Lenters, J.D., Cook, K.H., 1999. Summertime precipitation variability over South America: role of the large-scale circulation. Mon. Weather Rev. 127, 409–431.
Magrin, G.O., Travasso, M.I., Rodriguez, G.R., 2005. Changes in climate and crop production during the 20th century in Argentina. Clim. Change 72, 229–249.
Moriasi, D.N., Arnold, J.G., Van Liew, M.W., Bingner, R.L., Harmel, R.D., Veith, T.L., 2007. Model evaluation guidelines for systematic quantification of accuracy in watershed simulations. Am. Soc. Agric. Biol. Eng. 50, 885–900.
Morton, F.I., 1983. Operational estimates of lake evaporation. J. Hydrol. 66, 77–100.
Nachtergaele, F., van Velthuizen, H., Verelst, L., 2009. Harmonized World Soil Database, Version 1.1. FAO, Rome, Italy and IIASA, Laxenburg, Austria.
Nash, J.E., Sutcliffe, J.V., 1970. River flow forecasting through conceptual models part I – a discussion of principles. J. Hydrol. 10, 282–290.
Neitsch, S.L., Arnold, J.G., Kiniry, J.R., Williams, J.R., King, K.W., 2002. Soil and Water Assessment Tool Theoretical Documentation. Version 2000. Texas Water Resources Institutes, College Station, Texas, USA.
Pasquini, A.I., Lecomte, K.L., Piovano, E.L., Depetris, P.J., 2006. Recent rainfall and runoff variability in central Argentina. Quatern. Int. 158, 127–139.
Paulhus, J.L.H., Kohler, M.A., 1952. Interpolation of missing precipitation records. Mon. Weather Rev. 80, 129–133.
Piovano, E.L., Ariztegui, D., Córdoba, F., Cioccale, M., Sylvestre, F., 2009. Hydrological variability in South America below the Tropic of Capricorn (Pampas and Patagonia, Argentina) during the last 13.0. In: Vimeux, F. et al. (Eds.), Past Climate Variability in South America and Surrounding Regions: From the Last Glacial Maximum to the Holocene. Developments in Paleoenvironmental Research Series (DPER), pp. 323–351.
Prohaska, F., 1976. The climate of Argentina Paraguay and Uruguay. World Survey of Climatology. Clim. Central South America 12, 13–112.
Qian, T., Dai, A., Trenberth, K.E., Oleson, K.W., 2006. Simulation of global land surface conditions from 1948 to 2004. Part I: forcing data and evaluations. J. Hydrometeorol. 7, 953–975.
Sankarasubramanian, A., Vogel, R.M., Limbrunner, J.F., 2001. Climate elasticity of streamflow in United States. Water Resour. Res. 37, 1771–1781.
Schuol, J., Abbaspour, K.C., Srinivasan, R., Yang, H., 2008. Estimation of freshwater availability in the West African Sub-continent using the SWAT hydrologic model. J. Hydrol. 352, 30–49.
Setegn, S.G., Srinivasan, R., Melesse, A.M., Dargahi, B., 2010. SWAT model application and prediction uncertainty analysis in the Lake Tana Basin, Ethiopia. Hydrol. Process. 24, 357–367.
SCS (Soil Conservation Service), 1972. National Engineering Handbook, Section 4. US Department of Agriculture, Washington, DC.
Sharpley, A.N., Williams, J.R., 1990. EPIC – Erosion/Productivity Impact Calculator; 1. Model Documentation. Technical Bulletin 1768. US Department of Agriculture.
Shrestha, S., Bastola, S., Babel, M.S., Dulal, K.N., Magome, J., Hapuarachchi, H.A.P., Kazama, F., Ishidaira, H., Takeuchi, K., 2007. The assessment of spatial and temporal transferability of a physically based distributed hydrological model parameters in different physiographic regions of Nepal. J. Hydrol. 347, 153–172.
Stehr, A., Debels, P., Romero, F., Alcayaga, H., 2008. Hydrological modeling with SWAT under conditions of limited data availability: evaluation of results from a Chilean case study. Hydrol. Sci. J. 53, 588–601.
Troin, M., Vallet-Coulomb, C., Sylvestre, F., Piovano, E., 2010. Hydrological modelling of a closed lake (Laguna Mar Chiquita, Argentina) in the context of 20th century climatic changes. J. Hydrol. 393, 233–244.
van Griensven, A., Francos, A., Bauwens, W., 2002. Sensitivity analysis and autocalibration of an integral dynamic model for river water quality. Water Sci. Technol. 45 (9), 325–332.
van Griensven, A., Meixner, T., Grunwald, S., Bishop, T., Di Luzio, M., Srinivasan, R., 2006. A global sensitivity analysis method for the parameters of multi-variable watershed models. J. Hydrol. 324, 10–23.
Winchell, M., Srinivasan, R., Di Luzio, M., Arnold, J., 2007. ArcSWAT Interface for SWAT 2005. User's Guide, pp. 1–436.